Microbially Deposited Manganese and Iron Oxides on Passive Metals—Their Chemistry and Consequences for Material Performance

X. Shi, R. Avci,** and Z. Lewandowski****

ABSTRACT

The open-circuit potential (OCP) values of Type 316L (UNS S31603) stainless steel and Ti-6Al-4V (UNS R56400) corrosion coupons, exposed to fresh river water, were ennobled to as high as 365 mV vs saturated calomel electrode (SCE) and 400 mV_{SCE}, respectively. With microchemical imaging capabilities and high-detection sensitivity, a surface analysis technique based on time-of-flight secondary ion mass spectroscopy (ToF-SIMS) was developed to identify the oxidation states and distribution of biominerals on the ennobled metal surfaces. ToF-SIMS spectra of the microbial deposits compared to spectra of different manganese and iron mineral standards indicated that the biominerals on the metal surfaces are a mixture of ferric oxide (Fe_2O_3), manganese oxide (Mn_3O_4), and manganese oxyhydroxide (MnOOH) on fully ennobled coupons, and a mixture of iron oxide (Fe_3O_4), Fe_2O_3, Mn_3O_4, and manganese(III) oxide (Mn_2O_3) on partially ennobled coupons. Biomineralized manganese and iron oxides on the Type 316L stainless steel surfaces, regardless of the oxidation states, endanger the material integrity in a similar manner, as evidenced by the elevated OCP and increased cathodic current density upon mild polarization.

KEY WORDS: biofilm, biomineralization, ennoblement, manganese oxidizing bacteria, microbially influenced corrosion, surface analysis, time-of-flight secondary ion mass spectroscopy, Type 316L stainless steel

INTRODUCTION

Microbially deposited minerals on water-immersed metal surfaces play an important role in microbiologically influenced corrosion (MIC).[1-7] Therefore, identifying the active biomineralization processes that occur on the metal surfaces in natural waters provides a convenient point of departure to study MIC and general metal/microbe interactions. For example, the corrosion mechanisms of mild steel, modified by the presence of sulfate-reducing bacteria (SRB), and corrosion of stainless steel (SS), modified by the presence of manganese-oxidizing bacteria (MOB),[3] demonstrate that the nature of MIC in both cases depends on the chemical composition of inorganic materials precipitated at the metal surface: iron sulfides and manganese oxides. These minerals, which are electrochemically active and are in electrical contact with the surface, modify electrochemical processes that naturally occur at the metal/solution interface and, therefore, accelerate corrosion. Practical effects of biomineralization on corrosion may be exemplified by the failure of Type 304L (UNS S30403)[(1)] piping at the Robinson Nuclear Power Station after a 13-year exposure to untreated water containing only 3 ppm chloride and 6 ppm sulfate.[8] The inner surfaces of the pipes were covered with 1/4-in.- (6.35-mm)-thick microbial deposits contain-

Submitted for publication November 2001; in revised form, February 2002. Presented as paper no. 456 at CORROSION/2002, April 2002, Denver, CO.

* Center for Biofilm Engineering, Montana State University, Bozeman, MT 59717-3980.
** Image and Chemical Analysis Laboratory, Department of Physics, Montana State University, Bozeman, MT 59717-3980.
*** Center for Biofilm Engineering and Department of Civil Engineering, Montana State University, Bozeman, MT 59717-3980.

(1) UNS numbers are listed in *Metals and Alloys in the Unified Numbering System*, published by the Society of Automotive Engineers (SAE) and cosponsored by ASTM.

0010-9312/02/000159/$5.00+$0.50/0

ing 37 wt% manganese, and the mechanism of accelerated corrosion was attributed to MOB activity.

Recent studies have demonstrated that biomineralization of manganese is responsible for the ennoblement of SS, one of the most puzzling phenomena associated with MIC. Ennoblement, a subject of continual controversy since its discovery,[9-16] features microbial colonization of passive metals followed by an increase in the open-circuit potential (OCP), reaching final values between 200 mV vs saturated calomel electrode (SCE)[11] and 450 mV_{SCE},[9,13] accompanied by an increase in cathodic current density upon mild polarization of the ennobled samples.[16] In some instances and for some materials, the ennobled OCP approaches the critical pitting potential of the passive metal, which increases the risk of localized corrosion. As an example, turbine runner blades in a hydroelectric power plant were severely damaged.[17-18] The mechanism of the material failure was not immediately obvious because the chloride concentration in the water (20 mg/L to 170 mg/L) was not high enough to cause pitting of the turbine material (13%Cr-4%Ni). Scanning electron microscopy/energy dispersive x-ray analysis (SEM/EDAX) and x-ray diffraction analyses of deposits removed from the corroded blades showed the presence of manganese-containing minerals (≈ 25 wt% manganese oxyhydroxide [MnOOH] and 8 wt% manganese dioxide [MnO_2]), and the deposits had a high OCP (570 mV vs standard hydrogen electrode [SHE]), characteristic of ennoblement. It was concluded that the high OCP was caused by the reduction of MnO_2 to Mn^{2+}.

Dickinson and coworkers studied the effects of MOB on SS and demonstrated that 3% to 5% surface coverage by biofouling deposits was enough to ennoble the potential of Type 316L (UNS S31603) SS.[19-20] Chemical examination of the deposits showed the presence of Fe(III) and Mn(IV),[16] while epifluorescence microscopy revealed the presence of manganese- and iron-oxidizing bacteria. Based on these observations and other studies, it is believed that the MOB involvement in corrosion of SS is based on the following mechanism:[21-24] the Mn^{2+} ions are microbially oxidized to MnOOH, which is deposited on the metal surface, then the solid MnOOH is further microbially oxidized to MnO_2. Both reactions contribute to the increase in the OCP because the deposited oxides, MnOOH and MnO_2, are in electrical contact with the surface and their dissolution potential is determined by the equilibrium of deposited minerals with the dissolved Mn^{2+}. The oxides, deposited on the surface, are reduced to the Mn^{2+} by electrons generated at anodic sites. However, reducing the manganese oxides does not stop the ennoblement process because the reduced products of this reaction, soluble Mn^{2+} ions, are reoxidized by the MOB attached to the metal surface. The described sequence of events, oxidation-reduction-oxidation of manganese, is a hypothetical mechanism that produces renewable cathodic reactants, MnOOH and MnO_2, and their presence on the metal surface endangers material integrity.

This hypothetical mechanism has been partially verified by defining surface chemistry of the microbial deposits and demonstrating, under well-defined laboratory conditions, that Type 316L SS exposed to MOB (*Leptothrix discophora* SP-6) in a mineral-salt-pyruvate-vitamin medium containing Mn^{2+} ennobled to the same extent as the coupons exposed to natural waters. The coupons ennobled under well-defined laboratory conditions exhibited electrochemical characteristics, in terms of OCP and potentiodynamic polarization plots, almost identical to the corrosion coupons ennobled in natural waters.[23] However, this was just a laboratory study, and the results had to be corroborated by field studies before concluding that such a mechanism is indeed active in natural waters. The difficulty with conducting field studies to verify the hypothesis is in examining the chemistry of the microbial deposits, which are more complex than the deposits from laboratory studies. Before drawing definite conclusions, suitable analytical techniques had to be used to demonstrate the sequence of chemical transitions on metal coupons exposed to natural waters. This paper describes the efforts toward adapting time-of-flight secondary ion mass spectroscopy (ToF-SIMS) as a surface analytical technique suitable for analyzing the biomineralized deposits on SS exposed to natural waters. This technique was used to test the hypothesis proposed in the present laboratory studies.

The chemistry of microbial deposits on solid surfaces is difficult to define—different microorganisms seem to deposit different minerals, and the deposited minerals are not stable. Instead, their chemistry can change with time. For example, Mn oxides formed by different *Bacillus spp.* and sheathed *Leptothrix* resemble vernadite, δ-MnO_2, whereas a microalga, *Chlamydomonas*, deposits manganite (γ-MnOOH).[25] As time progresses, the compositions of the deposits change. An amorphous Mn oxide deposited by a marine *Bacillus sp.* (SG-1) later recrystallized to hausmannite (Mn_3O_4),[25] and the octahedral hausmannite formed by the SG-1 spores aged to MnO_x (x = 1.9) over a period of weeks.[26] It has been suggested that the biomineralized manganese is a mixture of birnessite and pyrolusite (MnO_2), γ-MnOOH, and other oxides, and that microbial deposits typically have highly disordered structures.[27] The analysis of the microbial deposits on surfaces of field-ennobled Type 316L SS coupons using x-ray photoelectron spectroscopy (XPS) revealed a mixture of different manganese minerals with the chemistry not clearly identified.[21-22] The electrochemical analysis using cyclic voltammetry[5] detected MnO_2 in the biomineralized manganese oxides formed on metal

surfaces in natural waters, but failed to identify other phases.

The authors' laboratory experiments have dealt entirely with MOB and biomineralized manganese oxides. However, it is well known that biomineralized deposits in natural waters are usually manganese deposits mixed with iron deposits. Also, the biomineralized iron oxides as well as manganese oxides have been implicated in MIC: iron oxide formation could initiate under-deposit corrosion of susceptible metals.[3] In a failure case of Type 304L and Type 316L SS tanks and pipes that were partially filled with well water containing ~200 ppm chloride,[28] surface deposits contained manganese and iron and both iron-oxidizing bacteria (IOB) and MOB were identified. Therefore, iron oxides have to be included in any MIC-relevant description of chemistry of biomineralized deposits on SS in natural waters. Including iron oxides adds complexity to the already complicated problem, since the chemical composition of biomineralized iron deposits is at least as difficult to establish as it is to define that of biomineralized manganese deposits. Oxide films formed on iron in air consist of magnetite (Fe_3O_4) and hematite (Fe_2O_3).[4] Ferric oxyhydroxides, including goethite (α-FeOOH) and lepidocrocite (γ-FeOOH), have also been identified in protective layers on carbon steel. The Raman spectra of deposits obtained from Type 304L pipework that had failed by MIC in iron-rich potable water revealed the presence of a mixture of α-FeOOH and γ-FeOOH.[7] A simulation experiment indicated that FeOOH deposits can be chemically transformed, first to Fe_2O_3 and then to Fe_3O_4. Another complicating factor in the analysis of MIC-associated biomineralized oxides is the possible chemical reactions between manganese oxides and iron oxides.

As the surface analytical technique to analyze the biomineralized deposits, ToF-SIMS was used, which offers high-detection sensitivity and chemical imaging,[29-30] detects elements as well as chemical compounds, differentiates among isotopes, and allows mass imaging of deposits with submicron spatial resolution.[31] Using computerized data collection and retrospective analysis, the two-dimensional imaging of spatial distribution of chemical composition is possible. Due to its chemical imaging capabilities, SIMS has been applied to study the chemistry and distribution of oxides. For example, the distribution of ^{18}O, Fe, and Cr in an oxide scale grown on 9% Cr/Fe steel was obtained and found informative in understanding the corrosion mechanisms,[32] and depth profiling of oxide layers was performed to investigate a corroded zircaloy fuel rod cladding specimen.[31] In another case, the ratios MO_2^-/MO^- and MO_3^-/MO^- for transition metal oxides of the type M_xO_y were measured to identify their oxidation state. The data for iron oxide were then compared to those for the oxide found on a steel sample with an oxide film 4 nm thick, and the best match was to Fe_2O_3.[29] The authors have developed a technique based on ToF-SIMS to identify the biominerals on Type 316L SS and Ti-6Al-4V (UNS R56400) corrosion coupons ennobled by the biofilm of MOB, *Leptothrix discophora* SP-6.[24] The experimental results were statistically reproducible and the technique demonstrated reliable performance for surface sensitive analysis. It was found that the microbial deposits on ennobled coupons consist of MnOOH and MnO_2.

The mechanism of ennoblement failed to be verified by determining the chemical composition of microbial deposits on SS coupons because elements in the base metal, iron and manganese, had interfered with the secondary ion peaks in the SIMS spectra of microbial deposits on the ennobled coupons. For example, when the deposit-covered metal surface was sputtered by the primary ion of SIMS and produced ion fragments (secondary ions), MnH^+ from the microbial deposits could not be differentiated from MnH^+ and Fe^+ from the metal substratum. The extent of this interference was unknown because the authors did not have an independent standard to assess these contributions. To eliminate the effects of alloying elements, two types of coupons (Type 316L SS and low-iron titanium alloy [Ti-6Al-4V]) were used and exposed to the same environments. Assuming that the chemical nature of the deposits was the same on both coupons, any differences in the SIMS spectra would have to reflect the contribution of iron in the SS coupons. Implementing this strategy, the SIMS spectra of the deposits on the Ti-6Al-4V coupons were used to verify the conclusions obtained from analyzing the deposits on Type 316L SS coupons.

The goal of this work was to analyze the chemical composition of biomineralized manganese and iron deposited on passive metals in natural waters. A set of Type 316L SS and Ti-6Al-4V corrosion coupons were placed in a fresh water creek in Bozeman, Montana, for ennoblement. Then, the composition of the surface deposits was determined by comparing the SIMS spectra of the deposits with spectra of manganese standards (MnO_2, MnOOH, Mn_3O_4, MnO, manganese[III] oxide [Mn_2O_3], and manganese[II] carbonate [$MnCO_3$]) and iron standards (iron[II] oxide [FeO], Fe_2O_3, Fe_3O_4, and FeOOH). As a result, the chemistry of deposits and spatial distribution of microbially deposited minerals on the metal samples were defined. In addition, electrochemical techniques were applied to evaluate the consequences of depositing biomineralized manganese and iron oxides on the OCP and current density generated during potentiodynamic polarization of the ennobled coupons.

EXPERIMENTAL PROCEDURES

The following two types of corrosion coupons were used: Type 316L SS and Ti-6Al-4V, each 1.6 cm

TABLE 1
Elemental Composition of Type 316L SS Corrosion Coupons (wt%)

Fe	Cr	Ni	Mo	Mn	Si	P	N	C	S
Bal.	16.19	10.19	2.10	1.71	0.39	0.034	0.03	0.017	0.001

in diameter. Both materials were cut from larger metal sheets. Tables 1 and 2 show the composition of these materials as provided by the vendor. The coupons were polished, as described in a previous paper, to provide a mirror-finish surface sufficiently free of flaws for surface analyses.[24] Then, the coupons were sonicated, first in acetone (CH_3COCH_3) and then in 95% ethanol (C_2H_6O), each for 5 min, to remove any residual oil-based contamination. The coupons were air-dried and mounted in polycarbonate holders using a slow-hardening epoxy. Electrical connections were made to monitor OCP of the coupons by attaching conductive springs to the back of the coupons inside the holders. Prior to ennoblement experiments, the coupons were left in contact with atmospheric air for 24 h to form a protective surface layer of metal oxides.

For field exposure, a set of Type 316L SS and Ti-6Al-4V corrosion coupons were placed in Roskie Creek, a fresh water creek in Bozeman, Montana. This particular site has previously been classified as a clean stream.[20] As shown in Figure 1, the coupons were mounted in a polyvinyl chloride (PVC) frame and placed face down ~10 cm above the sediments. Electrical connections were extended 30 cm above the surface during the measurements and sealed in a waterproof bag between measurements. During 40 days of exposure, the setup and measured OCP were checked weekly against the SCE. During the time of exposure, the following parameters fluctuated within the boundaries indicated: 6.8 to 7.2 pH, 11°C to 18°C, 150 µS conductivity, 60 µg/L to 80 µg/L Mn^{2+}, 300 µg/L Fe^{3+}, and 8 mg/L to 9 mg/L dissolved oxygen.

For all electrochemical studies, a flat-type three-electrode electrochemical cell was used with a SCE and two high-density graphite counter electrodes. An EG&G model 273A[†] potentiostat/galvanostat was used, which was interfaced to and controlled by a computer using the EG&G Princeton Applied Research 352 SoftCorr III[†] corrosion measurement software.

To simulate the electrochemistry of SS surfaces covered with biomineralized manganese oxides, manganese dioxide was galvanostatically plated on Type 316L SS corrosion coupons. The coupons were electroplated in an aqueous electrolyte containing 0.1 M sodium sulfate (Na_2SO_4) and 5 mM manganese sulfate ($MnSO_4$) at pH 6.5, buffered by boric acid (H_3BO_3) and borate. A total charge of 30 mC/cm^2 was transferred at a rate of 0.01 mA/cm^2, corresponding to a 270-nm thick layer of solid MnO_2.

[†] Trade name.

TABLE 2
Elemental Composition of Ti-6Al-4V Corrosion Coupons (wt%)

Ti	Al	V	N	C	H	Fe	Mn	O
Bal.	6.0	4.0	0.05	0.1	0.012	0.3	0.01	0.2

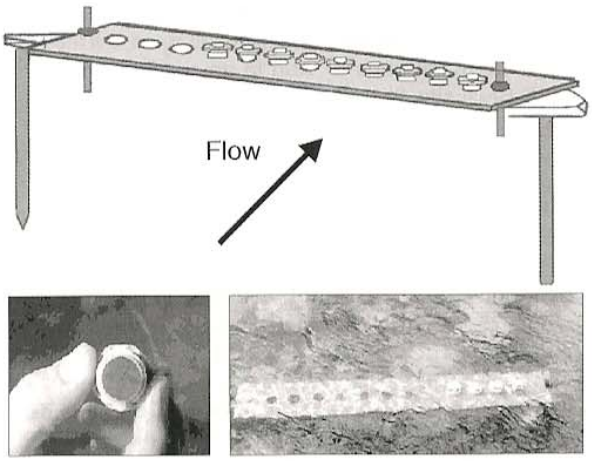

FIGURE 1. *Coupon holders and frames that were used to expose the SS coupons at the sampling sites. The corrosion coupons were mounted in threaded PVC plugs that were then screwed into frames constructed of 1/4-in. PVC sheets, 3 in. by 12 in. Coupon holders were fitted with nylon plugs that could be removed to allow access to the backside of the coupon for OCP measurements. Frames were held in place with steel spikes in the stream.*

To identify possible interactions between ferrous ion and manganese oxides on a SS surface, several MnO_2-plated SS coupons were immersed into an aqueous electrolyte containing 0.1 M Na_2SO_4, 2.5 mM ferrous sulfate ($FeSO_4$), and 1 mM $MnSO_4$, buffered by H_3BO_3 and borate at pH 6.8. During the 48-h immersion, the solution was purged with argon to avoid any possible involvement with oxygen. The coupons were then rinsed with distilled water and prepared for OCP measurements and surface analyses.

To evaluate the effects of biomineralized oxides on material integrity, the coupons before and after the ennoblement were potentiodynamicly polarized at room temperature in 0.01 M Na_2SO_4 solution buff-

ered to pH 8.30 using H_3BO_3 and borate and air-saturated by stirring vigorously at a constant rate. The coupon, which served as the working electrode, was cleaned with distilled water before mounting it to the electrochemical cell. The exposed area of the coupon was 1 cm^2. The coupon was immersed for 10 min before the potentiodynamic measurement started to equilibrate and stabilize the metal/solution interface. A cathodic polarization scan was performed potentiodynamicly at a scan rate of 0.167 mV/s. The starting potential was chosen just above the OCP of the working electrode and the scan was terminated at 0.85 V_{SCE}. Each measurement was repeated at least twice to verify reproducibility.

ToF-SIMS analyses of the coupons and oxide standards were conducted using a Phi-Evans TRIFT I[†] mass spectrometer.[31] The working principle of this system can be found in advanced texts on surface analytical techniques[31-33] and in an earlier publication.[24] Basically, ToF-SIMS is an imaging mass spectroscopy analysis, which allows a high-resolution mass spectroscopy and high-resolution chemical maps to be obtained. The analyses were accomplished by rastering a focused primary ion beam across the surface of interest while collecting secondary ions at each point.

A pulsed gallium liquid metal ion gun (LMIG) fired at 25 keV primary energy (corresponding to 22 keV impact energy), with a 10-kHz repetition rate, was used as the primary ion source. A multi-stop time-to-digital converter (TDC) recorded the time of flight of the ion fragments with a 138-ps precision. The LMIG pulse width was kept at <14 ns while the raster size of the beam varied from 80 μm^2 by 80 μm^2 to 240 μm^2 by 240 μm^2, the combination of which yielded ~1 mm spatial resolution while simultaneously detecting ion fragments with ~m/Δm ~2,000 mass resolution. In all of the ToF-SIMS acquisitions, the primary ion dose remained <10^{13} ions per cm^2, which is within the limit of static SIMS requirements. A beam of low-energy (<20 eV) electrons was fired intermittently to prevent charging of the sample. The data acquisition and analysis were performed using ToF-SIMS software.

To analyze the surface chemistry of electroplated coupons, the metal surface was rinsed carefully with distilled water to clean any soluble salt that may exist. To analyze the surface chemistry of the ennobled coupons, the biofilm was gently removed using acetone, distilled water, and a paper tissue. The coupons were then mechanically removed from the holders, air-dried, and kept in separate airtight containers for up to 24 h prior to SIMS analysis to ensure dryness. After the SIMS analysis, the deposits were carefully removed from each coupon by sanding the surface with 0.05 μm polishing powder and then rinsing with distilled water. The SIMS spectra of each coupon surface were collected again. The latter results were used as controls, reflecting the chemistry of the bare metal surface after ennoblement or electroplating.

Six manganese oxides were used as standards to collect their SIMS reference spectra. MnO_2, MnOOH, Mn_3O_4, and $MnCO_3$ were chosen because they are reportedly the predominant species of manganese oxides in natural waters.[22] In addition, MnO and Mn_2O_3 were chosen to include other oxidation states of manganese that could be present on the ennobled coupons. Five of the oxides were commercial products: MnO (99%), Mn_2O_3 (99%), MnO_2 (99%), Mn_3O_4 (97%), and $MnCO_3$ (99.9+%). The sixth was a natural sample of the mineral manganite (MnOOH) from Wards Natural Science Establishment, Inc.[2] The sample of MnOOH was cut, fractured, and immediately inserted into the analysis chamber in vacuum to minimize surface contamination. From the x-ray powder diffraction patterns, it was verified that the sixth sample was pure manganite (δ-MnOOH).[33] Four iron oxides were also used as standards to collect their SIMS reference spectra: FeO (99.9%), Fe_2O_3 (99.999%), Fe_3O_4 (laboratory-grade), and FeOOH (99.8%). They make up the spectrum of possible states of biomineralized iron in the microbial deposits since no iron sulfides were identified.

The mineral standards for SIMS analysis were prepared by gently pressing the powdered compounds into a piece of soft indium foil using clean glass slides to ensure that the surface to be analyzed was flat. As a result, the sample spectra included a peak from indium, but this did not interfere with any peaks of importance for this study.

Since the microbial deposits were not uniformly distributed on the surface, the areas that were not covered by deposits needed to be eliminated to determine the composition of the deposits only. The raw data acquisition of ToF-SIMS stores a complete mass spectrum for each of the 256 pixels by 256 pixels uniformly distributed through the area of interest. Retrospective analysis of the raw SIMS data files makes it possible to obtain chemical maps of the specific ion fragments of choice. To determine the chemical composition of microbial deposits, the SIMS spectra is extracted using what is known as "region-of-interest" (ROI) acquisition during a retrospective analysis of "raw" data files.[31] An ROI was defined using a simple drawing tool to select the areas in a SIMS image from which mass spectra were acquired. This way the contributions from the bare surface are minimized.

RESULTS AND DISCUSSION

Chemical imaging capabilities of ToF-SIMS was used to study the surface chemistry of a MnO_2-plated

[2] Ward's Natural Science Establishment, Inc., PO Box 92912, Rochester, NY 14692-9012.

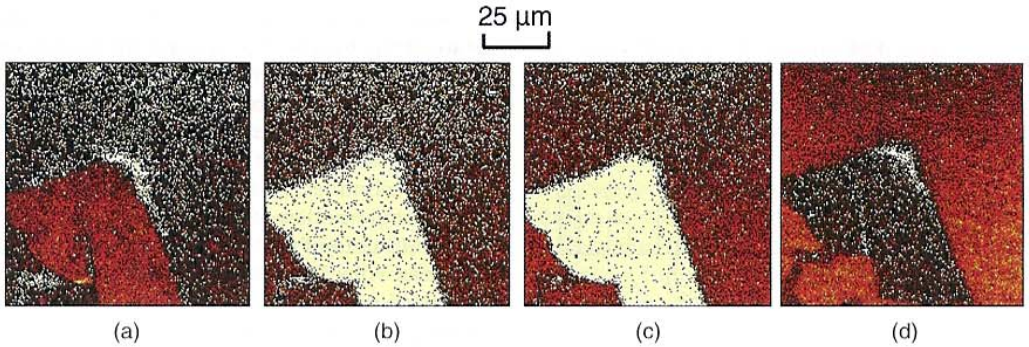

FIGURE 2. *ToF-SIMS images showing the distribution of secondary ions: (a) Mn^+, (b) FeH^+, (c) Cr^+, and (d) Fe^+. Data was collected from a 180-mm^2-by-180-mm^2 area on a Type 316L SS electroplated with MnO_2. The SIMS peak of Fe^+ was confounded by the presence of MnH^+. The white areas show low concentrations.*

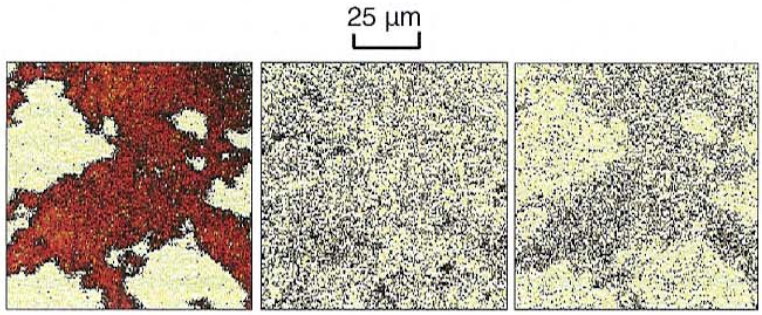

FIGURE 3. *ToF-SIMS images showing the distribution of secondary ions: (a) Ti^+, (b) Mn^+, and (c) FeH^+. Data was collected from a 180-mm^2-by-180-mm^2 area on a Ti-6Al-4V coupon ennobled to 400 mV_{SCE} in the Roskie creek. The white areas show low concentrations.*

SS coupon by collecting SIMS data from a 180-µm^2-by-180-µm^2 area on the surface. Figure 2 shows the distribution of secondary ions (Mn^+, FeH^+, Cr^+, and Fe^+) corresponding to the peaks at certain atomic mass units (amu), ~55, 57, 52, and 56, respectively. For the SIMS images, different colors indicate different intensities of the specific secondary ion. In this paper, the black-and-white format was used (i.e., white color indicates low intensity; black color indicates high intensity). In the Mn^+ map, the strong signals in the black regions indicate the presence of a MnO_2 layer while the Mn^+ signals in other regions come from the SS itself. In the regions covered by MnO_2, both FeH^+ and Cr^+ were depleted while Fe^+ appeared to be still present, but as explained below, this mass (56 amu) was mostly due to MnH^+ rather than Fe^+. The identification of the SIMS peaks of interest were as follows: Mn^+ (~55 amu), FeH^+ (~57 amu), and Cr^+ (~52 amu). The Fe^+ map suggests that the peak at ≈56 amu was actually the result of the presence of both Fe^+ and MnH^+. Therefore, in the regions covered by MnO_2, the signals were actually MnH^+, not Fe^+. For this reason, FeH^+ was used instead of Fe^+ to map the distribution of iron minerals on the metal surface. For cases where both Mn and Fe contributions were present simultaneously, a multivariable regression analysis technique was developed, as described in the Appendix to separate the Fe^+ and MnH^+ components of a peak at 56 amu.

With the imaging capabilities of ToF-SIMS, chemical maps of spatial distribution of the secondary ions of interest were generated on the surface of a Ti-6Al-4V coupon ennobled to 400 mV_{SCE} in the creek. The coupon was cleaned carefully with distilled water and paper tissue such that part of the biofilm and most of the biominerals were kept on the surface. Figure 3 shows the distributions of secondary ions (Ti^+, Mn^+, and FeH^+) on the Ti-6Al-4V coupon, which were generated from the same 180-µm^2-by-180-µm^2 area. FeH^+, instead of Fe^+, was used to map the distribution of iron oxides, because the latter could not be separated from the signals of MnH^+ in the SIMS spectra without numerical analysis. In the Ti^+ map, the depleted signals in the white regions indicated that they were covered by the residual biofilm, while the strong signals in the black regions indicated the absence of biofilm. In the regions not covered by the biofilm, both Mn^+ and FeH^+

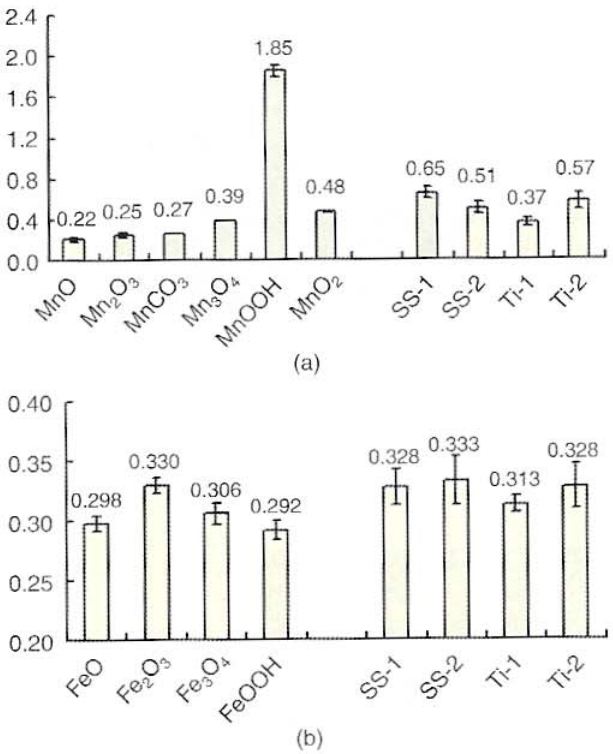

FIGURE 4. *Intensity ratios of secondary ions in the SIMS spectra as a function of oxide standards and unknown minerals on various ennobled coupons: (a) MnH^+/Mn^+ and (b) FeH^+/Fe^+. The ratios, with mass spectroscopy and chemical map information provided by the SIMS analysis, suggest that the biomineralized manganese on fully ennobled Type 316L SS (SS-1, SS-2: 365 mV_{SCE}) and Ti-4Al-6V (Ti-2: 400 mV_{SCE}) surfaces is a mixture of MnOOH and Mn_3O_4, whereas the biomineralized iron is mostly Fe_2O_3. For the partially ennobled Ti-4Al-6V (Ti-1: 350 V_{SCE}) surface, the biomineralized manganese is a mixture of Mn_3O_4 and Mn_2O_3, and the biomineralized iron is Fe_3O_4, mixed with a certain amount of Fe_2O_3.*

were enriched, which could be attributed to the presence of microbial deposits (enriched with Mn and Fe) and Fe in the metal substratum. In the regions covered by biofilm, however, Mn^+ was significantly enriched and FeH^+ was also present while Ti^+ was depleted. This was an expected result because Ti^+ came from the metal substratum only while the Mn^+ and FeH^+ signals came from the microbial deposits. Therefore, it was hypothesized that there was biomineralized manganese as well as iron in the biofilm and microbial deposits, which was confirmed by the quantitative ROI analyses. The semi-quantitative analysis in terms of areas under the peaks of the SIMS spectra further suggested that the amount of biomineralized manganese was higher than that of iron minerals in the biofilm.

As demonstrated by previous ToF-SIMS studies of microbial deposits on metal coupons ennobled under well-defined laboratory conditions,[24] there is a clear relationship between the ratios of certain signal intensities in the SIMS spectra and the oxidation state of the oxides. The relative intensities of the secondary ions can thus be used to identify the oxidation state of each oxide. This technique can be applied to identify unknown manganese oxides and iron oxides deposited on the metal surfaces. For a mixture of minerals, it is also possible to determine the mixing fraction of each oxide by making use of the SIMS data of well-defined standards and by using the lever rule: $R = xR_1 + (1 - x)R_2$, where R_1 and R_2 are standard ratios, R is the measured ratio, and x is the mixing fraction of oxide 1.

To identify various oxides and to quantify their observed differences, two groups of signal intensity ratios were used as indicators: MnH^+/Mn^+ and FeH^+/Fe^+ from the positive ion spectra. To achieve statistical reliability, the SIMS spectra were collected from 6~7 different areas on each sample (manganese/iron standards or metal coupons), and then the mean value and subsequently the standard deviation of the ratios were calculated using the procedure developed, as explained in the Appendix. Ratios from the negative ion spectra, such as $MnOH^-/MnO^-$ and $FeOH^-/FeO^-$, were less accurate, mostly likely because of low signal levels and the interference of organics left on the metal surface and, thus, were only used as additional information for confirmation.

In the SIMS analysis of the ennobled coupons, the signals of Mn^+ and $Fe^+ + MnH^+$ from the metal substratum contributed to those from the microbial deposits that the authors aim to identify. This contribution was eliminated by collecting SIMS spectra from both the ennobled coupon and the metal surface with microbial deposits removed. As described below, the contribution from the bare metal substratum was subtracted off and the difference was used as the signal from the microbial deposits alone. To determine the substrate contribution for Type 316L SS, Cr^+ was used as the internal intensity reference peak for normalization purposes, assuming it was not influenced by the microbial activities. The normalized substratum contributions were subtracted from the SIMS counts to determine the signals caused by the biominerals. Similarly, for Ti-6Al-4V, Ti^+ was used as the internal reference peak for normalization. In the Appendix, an example is given of the typical procedure for performing background subtraction and subsequent multivariable regression analysis technique to separate the MnH^+ and Fe^+ components of the peak at 56 amu to determine the true MnH^+/Mn^+ and FeH^+/Fe^+ ratios as a result of biominerals. The results of such analysis are described below. Figures 4(a) and (b) show the appropriate MnH^+/Mn^+ and FeH^+/Fe^+ intensity ratios, respectively, as a function of six manganese oxide standards (Figure 4[a]), and four iron oxide standards (Figure 4[b]), and as a function of samples: a partially ennobled Ti-6Al-4V (Ti-1: 350 mV_{SCE}), a fully

ennobled Ti-4Al-6V (Ti-2: 400 mV_{SCE}), and two ennobled Type 316L SS (SS-1, SS-2: 365 mV_{SCE}) coupons, where the extent of ennoblement was determined based on the potential.

The standard deviation of the intensity ratios relative to the mean values varied from 7% to 18%. The high standard deviations may have been caused by variations in the chemical composition of microbial deposits at microscopic scale and by variations in the chemical composition of the substratum from which the secondary ions were generated (matrix effect in the SIMS mechanism). For example, previous work using XPS analysis indicated that there were two or more manganese minerals with different oxidation states within the microbial deposits in natural waters.[22] In addition, the presence of organics may affect the secondary ion generation associated with the inorganic species. In spite of such uncertainties, the ToF-SIMS fragmentation patterns of manganese and iron standards are of great diagnostic value in determining the identification of inorganic microbial deposits on the ennobled or partially ennobled surfaces with reasonable confidence and accuracy.

The intensity ratio of MnH^+/Mn^+ in the SIMS data can be used to identify the oxidation state of biomineralized manganese. As shown in Figure 4(a), the mean values of MnH^+/Mn^+ in the SIMS spectra of biominerals on SS-1, SS-2, and Ti-2 (0.65, 0.51, 0.57) appears to lie between that of Mn_3O_4 (0.39) and MnOOH (1.85), as well as between MnO_2 (0.48) and MnOOH (1.85). Some individual observations on a number of spots revealed that MnH^+/Mn^+ ratios were <0.400 with no $MnCO_3$ identified in the SIMS spectra; therefore, the presence of Mn_3O_4 was expected. Based on the comparison of the two Ti-6Al-4V coupons, where the partially ennobled coupon had a lower mean value of MnH^+/Mn^+ (0.37) than the fully ennobled one (0.57), the possibility of a mixture of MnO_2 and MnOOH was ruled out. It was hypothesized that the biomineralized manganese on ennobled coupons was a mixture of Mn_3O_4 and MnOOH, perhaps mixed with very small amounts of MnO_2. The mean value of MnH^+/Mn^+ in the SIMS spectra of biominerals on Ti-1 (0.37) appeared to lie between that of Mn_2O_3 (0.25) and Mn_3O_4 (0.39). Since no $MnCO_3$ was identified in the SIMS spectra, it was concluded that the biomineralized deposits on the partially ennobled metal surface consisted of Mn_3O_4 and Mn_2O_3. As a result of MOB activities in natural waters, the manganese was expected to evolve from Mn^{2+} to Mn_3O_4 and Mn_2O_3, and then Mn_2O_3 transformed to MnOOH, and the OCP increased accordingly. It is interesting to note that the mechanism described as manganese biomineralization in natural waters is somewhat different from that observed in well-defined laboratory conditions. In the latter, the manganese biomineralization by *Leptothrix Discophora* SP-6 occurs in two steps:[24] first, Mn^{2+} is oxidized to MnOOH; then, MnOOH is further oxidized to MnO_2. Both mechanisms, however, were at least partly responsible for the observed OCP increase during the ennoblement process. The difference in manganese biomineralization can be explained by the presence of various types of microorganisms in natural waters including bacteria, yeast, and fungi. In addition, it was observed that the extracellular polymer substances (EPS) in natural waters were much more adherent to the metal surface and thus hypothesized that EPS played an important role in the ennoblement process in natural waters.

The intensity ratio of FeH^+/Fe^+ in the SIMS data, too, can be used to identify the oxidation state of biomineralized iron. As shown in Figure 4(b), the mean value of FeH^+/Fe^+ in the SIMS spectra of microbial deposits on SS-1, SS-2, and Ti-2 (0.33) is close to that of Fe_2O_3 (0.33). Therefore, it was hypothesized that the biomineralized iron on ennobled coupons was mainly Fe_2O_3. The mean value of FeH^+/Fe^+ in the SIMS spectra of microbial deposits on Ti-1 (0.313) was between that of Fe_3O_4 (0.306) and Fe_2O_3 (0.330). Given the uncertainties in these ratios, the two values were indistinguishable. Based on the thermodynamics, it was hypothesized that the biomineralized iron on partially ennobled metal surfaces consisted of Fe_3O_4 and Fe_2O_3. As the OCP increased, the iron evolved from a lower oxidation state to higher ones (i.e., from Fe^{2+} to Fe_3O_4, then to Fe_2O_3), as a result of IOB activities or simply because of the OCP increase caused by MOB activities.

To simulate the coexistence of manganese and iron oxides, experiments were conducted by immersing MnO_2-plated SS coupons into the solution of Fe^{2+} (2.5 m M $FeSO_4$). It was noted that the immersion did not cause any apparent change in the OCP of the metal samples, which stayed at ~ 360 mV_{SCE} in a solution of pH 7.2 and Mn^{2+} concentration of 1 by 10^{-6} M. The surface chemistry was analyzed before and after the immersion using ToF-SIMS. The mean value of MnH^+/Mn^+ of the surface deposits on the SS coupons before and after immersion was 0.43 and 1.12, respectively, which indicates a plated layer of MnO_2 (0.48) before immersion and a mixture of MnO_2 (0.48) and MnOOH (1.85) after immersion. The mean value of FeH^+/Fe^+ of the surface deposits on the SS coupons after immersion (0.35) indicates the formation of Fe_2O_3 (0.33). It was concluded that the MnO_2 deposited on SS coupons was reduced to MnOOH by oxidizing the Fe^{2+} to Fe_2O_3, indicating that the ferrous ion is a reductant of Mn(IV) oxides. In addition, the formed Fe_2O_3 seemed to be a stable product on the ennobled coupon and did not decrease the OCP of the coupon. Consequently, it was concluded that manganese oxides maintained the OCP of the metal coupons and the presence of iron oxides within the microbial deposits had little effect on the OCP of field-ennobled coupons.

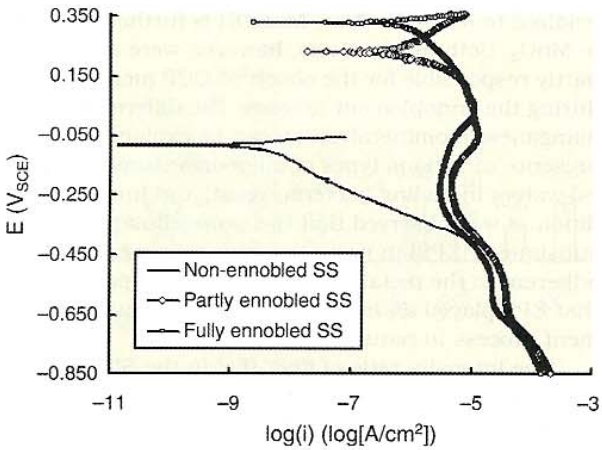

FIGURE 5. *Potentiodynamic polarization curves (obtained in 0.01 M Na_2SO_4 test solution, pH 8.30, scan rate: 0.167 mV/s) typical for SS coupons ennobled in the field to different degrees. The partially and fully ennobled SS coupons show a similar Tafel slope and similar cathodic current densities at modest overpotentials, even though the fully ennobled coupon has a higher corrosion potential. The curve corresponding to non-ennobled SS (solid line) is also shown for comparison.*

As a measure of material performance, the typical potentiodynamic polarization curves were obtained for non-ennobled, partially ennobled, and fully ennobled SS coupons, as shown in Figure 5. The partially and fully ennobled SS coupons had biofilm coverage of ≈100% and 95%, respectively, and the difference in coverage may reflect natural variations between the two coupons. Both partially and fully ennobled coupons shifted corrosion potentials several hundred millivolts in the noble direction. Polarization curves also show a corresponding increase in cathodic current density at modest overpotentials. For example, a 70-mV cathodic overpotential on non-ennobled coupons generates a current density of ~10^{-8} A/cm² while it generates a >2 orders of magnitude current density (~10^{-6} A/cm²) on fully ennobled coupons. The results are in accordance with previous publications,[19-20] which suggest that the increase in OCP and cathodic current density is most likely caused by the presence of microbially deposited oxides on the SS surface and indicates the decrease of corrosion resistance of the material. As shown in Figure 5, the polarization curves for partially and fully ennobled SS coupons show similar cathodic current behaviors during the cathodic polarization scan, whereas the fully ennobled coupon has a higher corrosion potential (0.330 mV_{SCE} vs 0.220 mV_{SCE}). The results suggest that biomineralized manganese and iron oxides on the Type 316L SS surfaces, regardless of their different oxidation states as indicated by the present SIMS analyses, impacted the material performance in a similar manner. Based on the present potentiodynamic polarization measurements, it was concluded that the biomineralized manganese and iron oxides deposited on the metal surface exhibited lower corrosion resistance and thus exposed a higher risk of localized corrosion. The possible correlation between the distribution of biomineralized manganese and iron oxides and that of localized corrosion is the subject of the authors' ongoing research.

CONCLUSIONS

❖ With microchemical imaging capabilities and high-detection sensitivity, a surface analysis technique based on ToF-SIMS was developed to identify the oxidation states and distribution of biominerals on Type 316L SS and Ti-6Al-4V corrosion coupons ennobled in natural waters. ToF-SIMS spectra of the microbial deposits compared to spectra of different manganese and iron mineral standards indicated that the deposits were a mixture of Fe_3O_4, Fe_2O_3, Mn_3O_4, and Mn_2O_3 on partially ennobled coupons, while a mixture of Fe_2O_3, Mn_3O_4, and MnOOH were found on fully ennobled coupons.

❖ The biomineralized manganese and iron oxides on Type 316L SS were responsible for the elevated OCP and corresponding increase in cathodic current density. Regardless of their oxidation states, the biomineralized oxides affected the material performance in a similar manner.

ACKNOWLEDGMENTS

This work was supported by the U.S. Office of Naval Research, contract no. N00014-99-1-0701 and by Cooperative Agreement EEC-8907039 between the National Science Foundation and Montana State University, Bozeman, Montana. The authors would like to acknowledge the ICAL facility of Montana State University for the use of XPS and ToF-SIMS.

APPENDIX

Table A-1 gives an example of determining the counts as a result of microbial deposits for seven different regions on the surface of an ennobled Ti-6Al-4V coupon, Ti-2 (ennobled to 400 mV_{SCE}). Columns 1 through 4 show the raw counts (areas under the peaks), I_T, of Mn^+, $MnH^+ + Fe^+$, FeH^+, and Ti^+. Columns 5 through 7 show the subtracted counts, I, as a result of biominerals. Columns 8 and 9 show the individual components, αI_1 (MnH^+) and βI_2 (Fe^+), of $MnH^+ + Fe^+$ (Column 6) determined by multiple regression. The sum of Columns 8 and 9 is roughly equal to Column 6 (Formula 2). The last row (ρ) shows the intensity ratios of Mn^+, $MnH^+ + Fe^+$, and FeH^+ to Ti^+ for the bare metal surface obtained after removing the biominerals from the ennobled coupon by means of polishing the surface very lightly. Also shown in this row are the parameters α and β, the

TABLE A-1

Example of Applying Equations (A-1) and (A-2) to Determine the Counts As a Result of Microbial Deposits and the True Ratios of MnH^+/Mn^+ and FeH^+/Fe^+

Region	(1) Mn^+	(2) $(MnH^+ + Fe^+)$[A]	(3) FeH^+	(4) Ti^+	(5) Mn^+	(6) $(MnH^+ + Fe^+)$[A]	(7) FeH^+[B]	(8) MnH^+	(9) Fe^+
1	1,731	4,189	1,072	26,358	1,656	3,930	937	1,069	2,986
2	35,623	97,481	28,317	515,981	34,157	92,417	25,635	14,156	72,947
3	47,443	122,043	31,758	732,775	45,361	114,851	28,012	29,334	88,995
4	14,344	21,964	4,428	746	14,342	21,957	4,138	9,324	13,782
5	6,207	8,921	1,803	307	6,206	8,918	1,678	3795	5,380
6	13,549	20,622	4,354	774	13,547	20,614	4,080	8,158	12,892
7	3,331	4,641	1,008	171	3,331	4,639	941	1,766	2,740
						$\alpha = 0.570 \pm 0.086$	$MnH^+/Mn^+ = 0.570 \pm 0.086$		
ρ	2.84×10^{-3}	9.81×10^{-3}	3.87×10^{-3}	1		$\beta = 3.053 \pm 0.055$	$FeH^+/Fe^+ = 0.328 \pm 0.018$		

[A] The two peaks cannot be resolved without numerical analysis.
[B] The counts due to MnH_2^+ were subtracted, the intensity of which was determined to be ~2% of Mn^+.

ratios MnH^+/Mn^+ and FeH^+/Fe^+, and their standard deviations.

Equation (A-1) is the relation used for subtracting background contributions:

$$I = I_T - \rho I_R \qquad (A\text{-}1)$$

In this formula, I represents the subtracted counts corresponding to Mn^+, $MnH^+ + Fe^+$, or FeH^+, attributed to the microbial deposits alone (Table A-1, Columns 5 through 7); I_T represents any of the total Mn^+, $MnH^+ + Fe^+$, or FeH^+ counts from the ennobled coupon, including those from the substratum surface and from the deposits (Table A-1, Columns 1 through 3); I_R is the counts of the reference peak from the ennobled coupon (Column 4), which was chosen to be Cr^+ or Ti^+, depending on whether a Type 316L SS or Ti-6Al-4V (as in example) was used as substrate; ρ is the mean value of the intensity ratios between Mn^+, $MnH^+ + Fe^+$, or FeH^+ of the bare metal surface and the reference peak, in the present case, Ti^+. These ratios are listed in the last row of Table A-1.

Column 6 of Table A-1 gives the background-subtracted peak intensity corresponding to $MnH^+ + Fe^+$, which contains contributions from both MnH^+ and Fe^+ ions. The basic approach here was to assume that the net $MnH^+ + Fe^+$ counts, I, from a given region as shown on Column 6, can be expressed as a linear combination of the net Mn^+ counts, I_1 (Column 5), and the net FeH^+ counts, I_2 (Column 7). This is supported by the fact that the FeH^+ peak does not receive much contribution from the manganese caused by the low MnH_2^+ yield. Experiments showed that this contribution was only ~2% of Mn^+ intensity and this value was subtracted from the raw FeH^+ intensity (Column 3). On the other hand, the MnH^+ comprised a substantial fraction of Mn^+ yield and could not be differentiated from Fe^+. Equation (2) is, in effect, a matrix equation correlating Column 6 to Columns 5 and 7 using two parameters, α and β:

$$I = \alpha I_1 + \beta I_2 \qquad (A\text{-}2)$$

where the coefficients α and β were determined applying the multivariable linear regression technique using the data listed in Columns 5 and 7.[34] Since there were two unknown parameters, α and β, data was collected from seven different regions on the surface of the same sample, Ti-2. Results of multiple regression analysis readily yielded $\alpha = 0.570 \pm 0.086$ and $\beta = 3.053 \pm 0.055$ (bottom row).

Using the α and β and Equation (A-2), the predicted contributions, αI_1 (MnH^+) and βI_2 (Fe^+), were calculated to the peak ~56 amu and the results are given in Columns 8 and 9, respectively. The mean values and the standard deviations of the ratios MnH^+/Mn^+ and FeH^+/Fe^+ could now readily be determined to be 0.570 ± 0.086 and 0.328 ± 0.018, respectively (bottom row). Since the standard deviations were within reasonable range, the ratios MnH^+/Mn^+ and FeH^+/Fe^+ were used to identify the oxidation state of biomineralized manganese and iron as discussed in the text.

REFERENCES

1. W.H. Dickinson, Z. Lewandowski, Biofouling 10 (1996): p. 79.
2. W.A. Hamilton, "Microbially Influenced Corrosion in the Context of Metal Microbe Interactions," in Biofilms: Recent Advances in Their Study and Control, ed. L.V. Evans (Amsterdam: Harwood Academic Publishers, 2000), p. 419-434.
3. Z. Lewandowski, W. Dickinson, W. Lee, Water Sci. Technol. 30, 1 (1997): p. 295.
4. B.J. Little, P.A. Wagner, Z. Lewandowski, "The Role of Biomineralization in Microbiologically Influenced Corrosion," CORROSION/98, paper no. 294 (Houston, TX: NACE International, 1998).
5. P. Linhardt, Mater. Sci. Forum 289-292 (1998): p. 1,267.
6. H. Volkland, H. Harms, B. Muller, G. Repphun, O. Wanner, A. J.B. Zehnder, Appl. Environ. Microbiol. 66, 10 (2000): p. 4,389.
7. I.G. Chamritski, G.R. Burns, B.J. Webster, N.J. Laycock, "Corrosion by Iron Oxidizing Bacteria: Model Development and Field Studies," CORROSION/2001, paper no. 254 (Houston, TX: NACE, 2001).
8. S.D. Strauss, Power 135 (1991): p. 50.
9. A. Mollica, A. Trevis, E. Traverso, G. Ventura, G. Decarolis, R. Dellepiane, Corrosion 45 (1989): p. 48.

10. V. Scotto, R. DiCintio, G. Marcenaro, Corros. Sci. 25, 3 (1985): p. 185.
11. R. Johnsen, E. Bardal, Corrosion 41, 5 (1985): p. 296.
12. S.C. Dexter, G.Y. Gao, Corrosion 44, 10 (1988): p. 717.
13. S. Motoda, Y. Suzuki, T. Shinohara, Corros. Sci. 31 (1990): p. 515.
14. P. Chandrasekaran, S.C. Dexter, "Mechanism of Potential Ennoblement in Passive Metals by Seawater Biofilms," CORROSION/93, paper no. 493 (Houston, TX: NACE, 1993).
15. M. Eashwar, S. Maruthamuthu, Biofouling 8 (1995): p. 203.
16. W.H. Dickinson, F. Caccavo, Jr., Z. Lewandowski, Corros. Sci. 38, 8 (1996): p. 1,407.
17. P. Linhardt, "Failure of Chromium-Nickel Steel in a Hydroelectric Power Plant by Manganese-Oxidizing Bacteria," in Microbially Influenced Corrosion of Materials, eds. E. Heitz, H.-C. Flemming, W. Sand (New York, NY: Springer Berlin Heidelberg, 1996), p. 221-230.
18. P. Linhardt, Werkst. Korros. 45 (1994): p. 79.
19. W. Dickinson, Z. Lewandowski, "Electrochemical and Microelectrode Studies of Stainless Steel Ennoblement," CORROSION/95, paper no. 223 (Houston, TX: NACE, 1995).
20. W. Dickinson, Z. Lewandowski, R.D. Geer, Corrosion 52, 12 (1996): p. 910.
21. B.H. Olesen, R. Avci, Z. Lewandowski, "Ennoblement of Stainless Steel Studied by X-Ray Photoelectron Spectroscopy," CORROSION/98, paper no. 275 (Houston, TX: NACE, 1998).
22. B.H. Olesen, R. Avci, Z. Lewandowski, Corros. Sci. 42, 2 (2000): p. 211.
23. W.H. Dickinson, F. Caccavo, Jr., B.H. Olesen, Z. Lewandowski, Appl. Environ. Microbiol. 63, 7 (1997): p. 2,502.
24. X. Shi, R. Avci, Z. Lewandowski, Corros. Sci. 44 (2003): p. 1,027.
25. A. Gounot, FEMS Microbiol. Rev. 14 (1994): p. 339.
26. K.H. Nealson, B.M. Tebo, R.A. Rosson, Adv. Appl. Microbiol. 33 (1988): p. 279.
27. R. Schweisfurth, G. Gattow, Z. Allg. Mikrobiol. 56 (1966): p. 303.
28. G. Kobrin, MP 7 (1976): p. 38.
29. N.M. Reed, J.C. Vickerman, "Static SIMS—Surface Analysis of Inorganic Materials," in Practical Surface Analysis, 2nd ed., eds. D. Briggs, M.P. Seah, vol. 2—Ion and Neutral Spectroscopy (New York, NY: John Wiley & Sons, 1996), p. 303-366.
30. S.S. Cristy, "Secondary Ion Mass Spectrometry," in Inorganic Mass Spectrometry: Fundamentals and Applications, eds. C.M. Barshick, D.C. Duckworth, D.H. Smith (New York, NY: Marcel Dekker, 2000), p. 159-221.
31. O. Gebhardt, Fresenius, J. Anal. Chem. 365 (1999): p. 117.
32. D. Briggs, A. Brown, J.C. Vickerman, Handbook of Static Secondary Ion Mass Spectrometry (New York, NY: John Wiley & Sons, 1990), p. 128-154
33. H.W. Nesbitt, D. Banerjee, Amer. Mineral. 83 (1998): p. 305.
34. C.R. Hicks, K.V. Turner, Fundamental Concepts in the Design of Experiments, 5th ed. (Oxford, U.K.: Oxford University Press, 1999), p. 424-430.